

# Effect of Rheological Properties on Power Consumption with Helical Ribbon Agitators

P. J. Carreau, R. P. Chhabra, and J. Cheng

Centre de Recherche Appliquée sur les Polymères (CRASP), Dept. of Chemical Engineering, Ecole Polytechnique, Montreal, Que., Canada H3C 3A7

*The influence of shear thinning and viscoelasticity on the power required for the mixing of viscous liquids using six different helical ribbon agitators has been investigated. Four Newtonian and 12 non-Newtonian fluids prepared using several polymers dissolved in varying concentrations in different solvents cover a wide range of rheological properties. By a careful choice of test media, the specific and combined effects of shear thinning and viscoelasticity on the power requirement have been examined. Simple models are proposed to predict the effective shear rate in the tank from the knowledge of the torque or power number. The effective shear rate predictions compared with the effective shear rate estimated using the scheme of Metzner and Otto (1957) show that they slightly depend on the shear thinning properties. Fluid's elasticity increases appreciably the power requirement, and departures from the generalized Newtonian power curve in the laminar regime are observed at smaller Reynolds numbers for viscoelastic fluids. Bottom wall resistance of the mixing vessel makes a negligible contribution to the power consumption.*

## Introduction

Mixing of liquids by mechanical agitation is a commonly encountered operation in chemical and polymer processing applications. Notwithstanding the importance of flow patterns, mixing time and so on, it is widely recognized that the power consumption is possibly the most important design parameter in these applications. Over the years, a wealth of information has accumulated on the power consumption for low viscosity liquids for a variety of geometrical configurations of agitator-tank combinations. Consequently, satisfactory methods are now available which permit the estimation of the power consumption for the mixing of low viscosity and purely viscous Newtonian and non-Newtonian systems under most conditions of practical interest. Excellent review articles are available on this subject (Oldshue, 1983; Ulbrecht and Carreau, 1985; Tattersson, 1991).

In contrast to this, the mixing of viscous non-Newtonian and rheologically complex media has received much less attention. The available scant literature on this subject has been reviewed by Ulbrecht and Carreau (1985) and Harnby et al. (1992). An examination of these reviews clearly suggests that the conventional impellers employed for the agitation of low

viscosity liquids are not at all satisfactory for the applications involving high viscosity liquids. It is now readily agreed that the close clearance type impellers (such as helical ribbon or screw) result in much better mixing and circulation. Detailed discussions concerning the relative merits and demerits of various impellers are also available in the literature (Tattersson, 1991). Among the different impeller geometries available, the helical ribbon agitator is considered to be more efficient for the agitation of highly viscous liquids. With this in mind, this article is concerned with the mixing of viscous Newtonian and non-Newtonian systems using a helical ribbon type agitator.

The power consumption is known to be strongly dependent upon the system geometry, type of agitator, the rheological characteristics of the liquid including shear thinning and viscoelasticity, and the kinematic conditions prevailing in the tank. Owing to the high viscosity of liquids being considered herein, the flow regime rarely exceeds beyond the transition zone between laminar and turbulent flows. It is well-known that strong interactions take place between the geometry and the viscoelasticity, and it is therefore not at all possible to extrapolate the role of viscoelasticity from one geometry to another, even qualitatively (Ulbrecht and Carreau, 1985). It is, therefore, not at all surprising that conflicting conclusions have been reached by different investigators regarding the pos-

Correspondence concerning this article should be addressed to P. J. Carreau.  
Present address of R. P. Chhabra: Indian Institute of Technology, Kanpur, India 208016

sible role of fluid viscoelasticity on power consumption. Admittedly detailed discussions concerning the influence of rheological complexities on power consumption are available in the literature (for example, Harnby et al., 1992); the salient features of the previous pertinent studies are recapitulated herein.

## Previous Work

Chavan and Ulbrecht (1973) developed a semi-theoretical model for the prediction of power for a helical screw in the laminar flow ( $Re < 10$ ) by assuming the flow to be a Couette type and by replacing the helical screw by an equivalent cylinder exerting the same torque. Their predictions for power law fluids are in agreement with the experimentally measured power data. Subsequently, Patterson et al. (1979) used the concept of drag flow about an inclined blade to predict the power, and the resulting expression was modified to include viscoelastic fluids (Yap et al., 1979). The Couette analogy approach has also been used to develop a theoretical framework for the prediction of the effective shear rate in the vessel (Ulbrecht and Carreau, 1985), albeit the predictions have not been validated thoroughly. Admittedly, some attempts have also been made at elucidating the effect of viscoelasticity on power consumption but conflicting conclusions have been reported in the literature. For instance, both Chavan and Ulbrecht (1973) and Yap et al. (1979) concluded that the shear thinning effects completely overshadowed viscoelastic effects for helical ribbon impellers. Whereas Nienow et al. (1983) reported a slight increase in power consumption for turbine impellers in viscoelastic xanthan gum solutions. In most of the aforementioned studies, aqueous polymer solutions (exhibiting both shear dependent viscosity as well as varying levels of viscoelasticity) have been used as model test fluids. It is thus not clear whether the observed changes in power consumption are due to the shear thinning, or due to the viscoelastic behavior or due to both. Subsequently, Prud'homme and Shaqfeh (1984) have used nonshear thinning but highly elastic fluids (Boger and Binnington, 1977) and reported a large increase in power consumption for turbine impellers. Similarly, very little is known about the influence of various geometric parameters such as the scale of equipment, bottom clearance, and so on on power consumption with helical ribbon agitators. Most of the previous work is limited to the so-called laminar flow regime and as far as known to us, no prior results on the mixing of viscoelastic systems with helical ribbon agitators in the transition zone are available in the literature. The present study aims to bridge this gap in our currently available body of knowledge.

In particular, this investigation sets out to elucidate the influence of fluid viscoelasticity and shear thinning on the effective shear rate and power consumption by using suitable and well characterized experimental fluids. Six helical ribbon-tank combinations have been used to demonstrate the effect of the equipment geometry on the power consumption. The experimental results reported herein embrace wide ranges of physical and kinematic conditions.

## Concepts

As suggested by Ulbrecht and Carreau (1985), the variation of power consumption with Reynolds number reflects the over-

all flow pattern and the *in situ* rheology of the mixed liquid in a mixing system. Dimensional analysis suggests that for purely viscous (that is, time-independent) fluids and in the absence of vortex formation, the power number is a unique function of Reynolds number as

$$Np = P/\rho N^3 d^5 = f(Re) \quad (1)$$

While for Newtonian systems the Reynolds number is defined unambiguously, considerable confusion exists regarding the appropriate choice of an effective viscosity for non-Newtonian fluids, since the deformation rate in a mixing vessel is neither constant nor is known *a priori*. This difficulty was circumvented by Metzner and Otto (1957) who introduced the concept of the effective shear rate, that is,

$$\dot{\gamma}_e = k_s N \quad (2)$$

where  $k_s$  is an experimentally determined constant and it is a function of geometry (see, for example, Takahashi et al., 1984). Though originally postulated to be independent of the liquid rheology, recent work, however, suggests that for shear thinning fluids its value also depends upon the power law index (Beckner and Smith, 1966; Yap et al., 1979; Brito et al., 1991). While Eq. 2 provides a convenient method for the estimation of power consumption for time-independent fluids, virtually no attempt has been made to delineate the variation of  $k_s$  with the power law index  $n$  and geometry. In the following section, simplified models are presented which do provide useful guidelines for calculating the effective shear rate for helical ribbon agitators operating in the laminar flow regime.

## Prediction of effective shear rate

A schematic representation of a helical ribbon agitator is shown in Figure 1. Following Bourne and Butler (1969), Chavan and Ulbrecht (1973) and Ulbrecht and Carreau (1985), the fluid motion caused by the rotating helical ribbon agitator is approximated here by an equivalent flow produced in a coaxial cylinder configuration with the inner cylinder rotating. The helical ribbon impeller is replaced by a cylinder of an equivalent diameter  $d_e$  which is rotating with a constant angular velocity  $\Omega$ . For steady and fully developed Couette flow and in the absence of end effects, one can postulate:

$$v_r = v_z = 0, \quad v_\theta = v_\theta(r) \quad (3)$$

$$\tau_{rz} = \tau_{\theta z} = 0, \quad \tau_{r\theta} = f(r) \quad (4)$$

The  $\theta$ -component of the motion equation simplifies to

$$\frac{\partial}{\partial r} (r^2 \tau_{r\theta}) = 0 \quad (5)$$

For power law fluids, the  $r\theta$ -component of the extra stress tensor may be expressed as

$$\tau_{r\theta} = -m \dot{\gamma}_{r\theta}^n = -m \left[ r \frac{\partial}{\partial r} \left( \frac{v_\theta}{r} \right) \right]^n \quad (6)$$

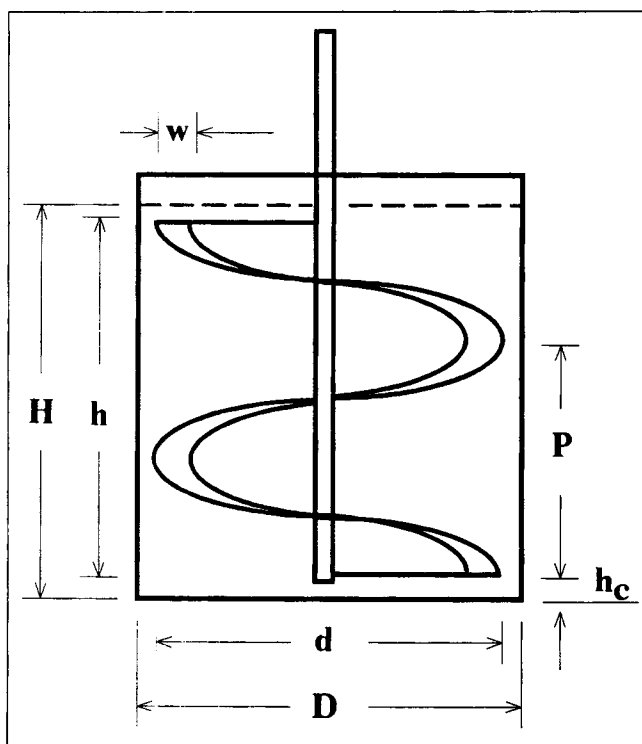


Figure 1. Sketch of helical ribbon agitator system.

Substituting Eq. 6 into Eq. 5 and integrating the resulting equation with respect to  $r$  and with the boundary conditions  $v_\theta = \Omega(d_e/2)$  at  $r = d_e/2$  and  $v_\theta = 0$  at  $r = D/2$  yields the following expression for the velocity profile:

$$\frac{v_\theta}{r} = \frac{\Omega}{[(D/d_e)^{2/n} - 1]} \left[ \left( \frac{R}{r} \right)^{2/n} - 1 \right] \quad (7)$$

Then from Eq. 6 the shear stress,  $\tau_{r\theta}$ , is given by

$$\tau_{r\theta} = m \left[ \frac{2\Omega}{n[(D/d_e)^{2/n} - 1]} \right]^n \left( \frac{R}{r} \right)^2 \quad (8)$$

The torque acting on the inner surface of outer cylinder is obtained from the wall shear stress

$$\Gamma = (2\pi RH) (-\tau_{r\theta})|_{r=R} \quad (9)$$

and the power required for mixing is

$$P = 2\pi\Gamma N \quad (10)$$

Then, combining Eqs. 8 to 10, the power number is expressed as:

$$Np = \frac{m\pi^2 D^2 H}{d^5 N^2 \rho} \left[ \frac{2\Omega}{n[(D/d_e)^{2/n} - 1]} \right]^n \quad (11)$$

In the laminar regime, the power number-Reynolds number relation can be expressed by

$$Np = K_p Re_g^{-1} = K_p \frac{\eta_e}{d^2 N \rho} \quad (12)$$

where  $\eta_e$  is an effective viscosity. For power law fluids,  $\eta_e = m|\dot{\gamma}_e|^{n-1}$  and Eqs. 11 and 12 can be rearranged to yield the following expression for the effective shear rate:

$$\frac{\dot{\gamma}_e}{N} = k_s = \left[ \frac{K_p d^3}{\pi^2 D^2 H} \right]^{\frac{1}{1-n}} \left[ \frac{n[(D/d_e)^{2/n} - 1]}{4\pi} \right]^{\frac{n}{1-n}} \quad (13)$$

Equation 13 thus elucidates the functional dependence of  $k_s$  on the flow behavior index  $n$  and geometry via  $d_e$ .

Alternately, one can rearrange Eq. 9 together with Eq. 6 to obtain the following expression for the shear rate at the outer cylinder, that is,  $\dot{\gamma}_{r\theta, \text{wall}}$  as

$$\dot{\gamma}_{r\theta, \text{wall}} = \left[ \frac{2\Gamma}{\pi m D^2 H} \right]^{1/n} \quad (14)$$

It can be argued that the effective shear rate  $\dot{\gamma}_e$  (estimated by using Eq. 13) and the shear rate at the wall  $\dot{\gamma}_{r\theta, \text{wall}}$  (calculated via Eq. 14) should be interrelated as both involve the knowledge of torque or power. The torque acting on the vessel wall can be represented as a function of the effective viscosity by combining Eqs. 10 and 12:

$$\Gamma_{\text{wall}} = \frac{K_p d^3 N}{2\pi} \eta_e \quad (15)$$

The wall shear rate is also assumed to be proportional to the rotational speed

$$\dot{\gamma}_{r\theta, \text{wall}} = k'_s N \quad (16)$$

where  $k'_s$  is a constant to be determined via the experimental results. For the power law fluids,  $\eta_e = m(k'_s N)^{n-1}$ , and from Eqs. 14 to 16,  $k_s$  can be expressed as a function of  $k'_s$ :

$$k_s = \left[ \frac{\pi^2 \left( \frac{D}{d} \right)^2 \left( \frac{H}{d} \right)}{K_p} \right]^{\frac{1}{n-1}} k'_s \frac{n}{n-1} \quad (17)$$

In contrast to Eq. 13, Eq. 17 can be used to predict  $k_s$  from  $k'_s$  without making use of the equivalent diameter,  $d_e$ .

## Experimental Studies

The mixing system employed in this work consisted of a cylindrical Plexiglas vessel fitted with a helical ribbon agitator together with an automated data acquisition system. In order to ascertain the effect of geometric parameters on power consumption, two cylindrical vessels (0.292 m and 0.40 m in diameter) together with six different helical ribbon agitators have been used; the major dimensions of the various tank/agitator combinations employed herein are defined in Figure 1, and their values are presented in Table 1. The torque acting on the agitator shaft was measured using a torque meter whereas the rotational speed was measured using a tachometer. More detailed descriptions of the experimental setup and procedure are available elsewhere (Carreau et al., 1976; Yap et al., 1979). It is sufficient to add here that each power data point represents an average of several repeated measurements in order to minimize the experimental uncertainty; the torque measurement is believed to be reproducible within  $\pm 2.0\%$ .

**Table 1. Geometrical Characteristics of Agitators**

Geometry	$d(m)$	$D/d$	$h/d$	$p/d$	$w/d$	$D/d_e^*$
HR1	0.263	1.11	1.05	0.695	0.097	1.42
HR2	0.263	1.11	1.05	0.850	0.133	1.50
HR3	0.263	1.11	1.05	0.695	0.133	1.37
HR4	0.360	1.11	1.03	0.686	0.083	1.45
HR5	0.360	1.11	1.03	1.030	0.133	1.57
HR6	0.360	1.11	1.03	0.686	0.133	1.43

\* $d_e$  calculated from Eq. 13 for Newtonian fluids ( $n = 1$ ).

### Test fluids

In order to encompass a wide range of the rheological characteristics, several Newtonian and non-Newtonian test fluids have been used in this work. Steady shear stress and primary normal stress differences were measured using a R-18 Weissenberg rheogoniometer at the same temperature as that encountered in the mixing experiments. Aqueous solutions of corn syrup (Bee Hive, Best Foods) and glycerol (G-177, American Chemicals) of different concentrations were used as Newtonian liquids whereas the non-Newtonian fluids used herein can be further divided into different types depending upon whether these fluids exhibited any measurable primary normal stress difference or shear dependent viscosity or both. Thus, the aqueous solutions of xanthan, XTN, (28602-8, Aldrich) and carboxyl methylcellulose, CMC, (CMC-70-F, Aqualon) and gellan (4900-1890, Scott) dissolved in a Newtonian corn syrup did not exhibit measurable primary normal stress differences and hence were classified as inelastic shear thinning fluids. On the other hand, solutions of xanthan and CMC in mixtures containing 85 mass % glycerol and 15 mass % water were found to be shear thinning as well as viscoelastic. Finally, the influence of viscoelasticity in the absence of shear thinning was examined by using two Boger fluids (Boger and Binnington, 1977). The first fluid was a 0.35% polyisobutylene, PIB, ( $M_w = 2.5 \times 10^6$  kg/kmol, Vistanex MM, Exxon) dissolved in a mixture containing 77 mass % of polybutene, PB, (Parapol 1300, Exxon) and 23 mass % kerosene, and the second fluid was a solution of 800 ppm of polyacrylamide, PAA, (Separan AP30, Dow Chemical) in corn syrup. This last fluid was slightly shear thinning.

Only steady-state shear viscosity and primary normal stress difference data were used to characterize the fluids. Owing to the qualitatively different behaviors, it was not possible to use a single rheological model even for their shear viscosity behavior. For instance, the usual two parameter power law model provides a satisfactory fit of the viscosity data for the aqueous solutions of xanthan and CMC as well as for the 0.7% gellan in corn syrup solutions. The more concentrated (1–3%) solutions of CMC, on the other hand, displayed a rather broad transition zone between the zero shear viscosity and power law regime. The Cross model was used to represent their shear viscosity-shear rate behavior:

$$\eta = \frac{\eta_0}{1 + (t_1 \dot{\gamma})^{n-1}} \quad (18)$$

For the solution of xanthan in the glycerol/water mixture, it was necessary to modify the power law by incorporating the solvent viscosity as follows

$$\eta - \eta_s = m |\dot{\gamma}|^{n-1} \quad (19)$$

The resulting values obtained by nonlinear regression of power law constants ( $n$  and  $m$ ), Cross model parameters ( $\eta_0$ ,  $n$  and  $t_1$ ) and the solvent viscosity  $\eta_s$  are given in Table 2 where a wide range of rheological conditions, especially the value of  $n$  (0.18 to 1.00), is seen to be covered. The solid curves in Figure 2 represent the fits obtained with the viscosity models.

The primary normal stress data are shown in Figure 3 to be adequately represented by the following power law type expression

$$N_1 = -(\tau_{11} - \tau_{22}) = \Psi_1 \dot{\gamma}^2 = m' / \dot{\gamma}^{n'} \quad (20)$$

and the experimental values of  $m'$  and  $n'$  are also included in Table 2. Attention is drawn to the fact that, as expected,  $n'$  is generally greater than the corresponding value of  $n$  and that the  $N_1$  data for the Boger fluids seem to approach the expected second-order limit and under these conditions, their viscoelastic behavior can be described in terms of a characteristic elastic time defined by

**Table 2. Rheological Parameters of the Fluids**

Fluids	$n$	$m$	$t_1$	$\eta_0$	$\eta_s$	$n'$	$m'$	$\rho$
	—	Pa·s <sup>n</sup>	s	Pa·s	Pa·s	—	Pa·s <sup>n'</sup>	kg/m <sup>3</sup>
Dilute corn syrup #1	1	12.0						1,440
Dilute corn syrup #2	1	4.16						1,360
Dilute glycerol #1	1	0.470						1,140
Dilute glycerol #2	1	0.067						1,100
2.5% XTN	0.183	22.4						1,080
0.5% XTN (gly./H <sub>2</sub> O)	0.199	4.13			0.19	0.782	7.85	1,200
1.8% XTN	0.200	11.8						1,080
0.8% XTN	0.240	2.31						1,050
0.5% XTN	0.250	1.84						1,030
3% CMC	0.299		7.83	469				1,060
1% CMC	0.409		0.110	1.57				1,040
0.4% CMC (gly./H <sub>2</sub> O)	0.530	9.75				0.740	18.0	1,200
0.1% CMC (gly./H <sub>2</sub> O)	0.701	1.20				1.12	0.140	1,200
0.7% gellan (corn syrup)	0.910	0.750						1,300
800 ppm PAA (corn syrup)	0.940	1.03				1.67	0.150	1,350
0.35% PIB (PB + Kerosene)	1	8.19				2.00	1.29	1,100

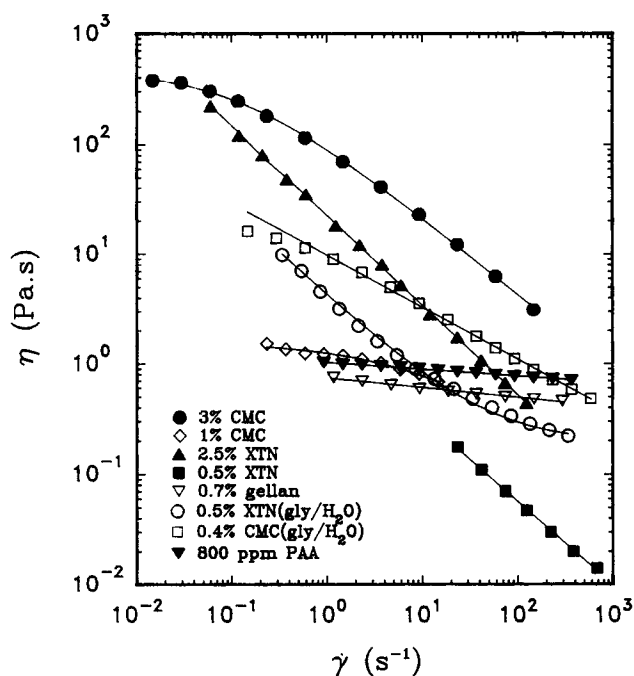


Figure 2. Shear viscosity data for eight polymer solutions.

$$\lambda = N_1 / 2\tau_{r0}\dot{\gamma}_{r0} \quad (21)$$

Figure 4 supports this contention whereas for all other fluids used herein, the characteristic elastic time decreases with increasing shear rate.

Thus, in this work, altogether 16 fluids exhibiting a wide range of rheological properties have been employed to delineate

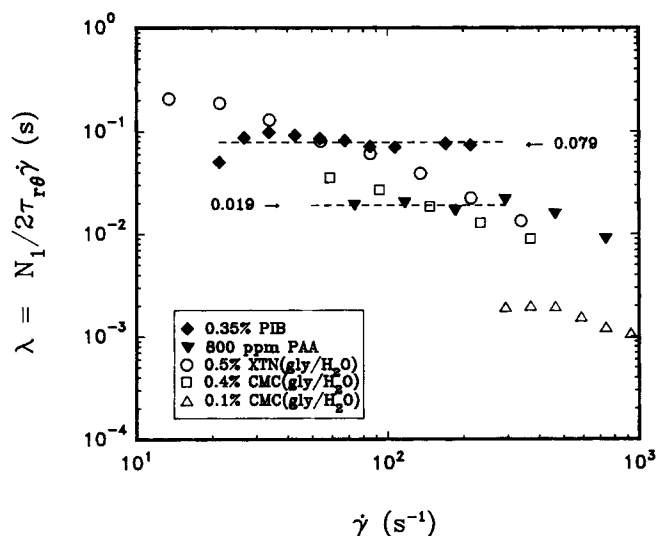


Figure 4. Variation of elastic time constant with shear rate for five polymer solutions.

the effects of non-Newtonian characteristics on the power consumption, and these are presented and discussed in the next section.

## Results and Discussion

The power consumption was measured as a function of the system geometry, rheological properties of fluids and kinematic variables, namely, speed. It is customary to present these results in a dimensionless form in terms of the power number as a function of the Reynolds number. It is desirable and instructive to begin with the results for Newtonian fluids, as it provides a convenient basis for the analysis of the results for the non-Newtonian systems (presented in subsequent sections).

### Newtonian liquids

The power consumption for Newtonian fluids has been measured using the six different agitators up to  $Re = 4,500$ , albeit our primary concern here is in the viscous and transition flow regimes. Depending upon the specific geometry of the agitator, the laminar flow regime ( $NpRe = \text{constant} = K_p$ ) is observed to persist up to about  $Re \approx 30 \sim 70$ , as shown by Figure 5. The critical value of the Reynolds number up to which the laminar flow prevails is seen to vary somewhat with the system geometry. The resulting mean values of  $K_p$  for all geometries are listed in Table 3. Also included in the same table are the calculated value of  $K_p$  using the semi-analytical methods due to Chavan and Ulbrecht (1973), Yap et al. (1979) and the empirical correlation proposed by Shamlou and Edwards (1985). While the agreement between the predicted and experimental values of  $K_p$  is seen to be moderately good for the models proposed by Chavan and Ulbrecht (1973) and by Yap et al. (1979), the correspondence with the results of Shamlou and Edwards (1985) is rather poor. Further examination of this table shows that the value of  $K_p$  increases with the decreasing agitator pitch and with the increasing blade width, albeit the latter is a rather small effect. These observations are

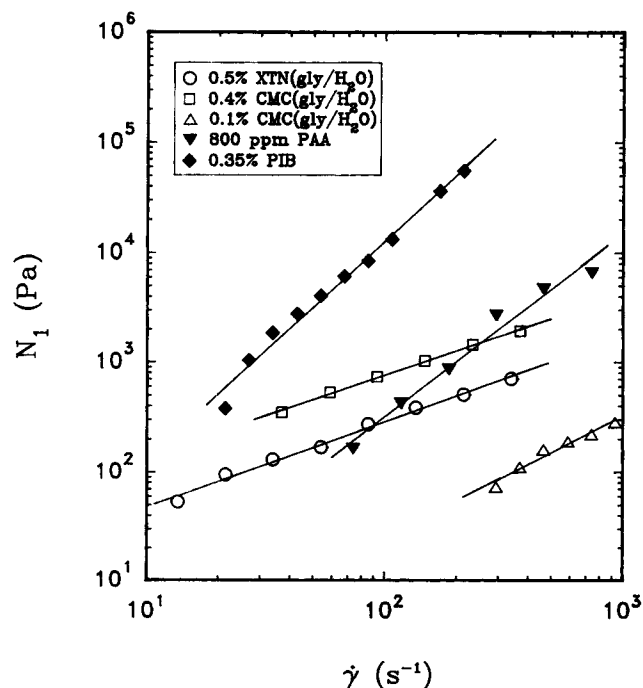
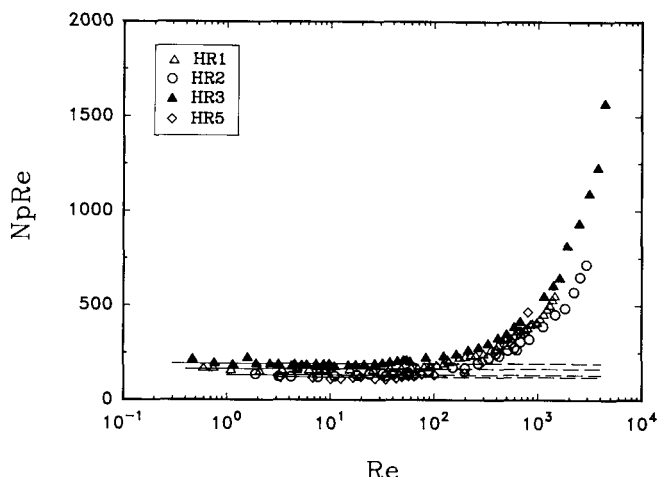


Figure 3. Primary normal stress difference data for five polymer solutions.



**Figure 5. Variation of  $NpRe_g$  with Reynolds number for Newtonian fluids.**

consistent with the findings of Hall et al. (1970), Chavan and Ulbrecht (1973) and Yap et al. (1979).

### Non-Newtonian fluids

Typical experimental results on power consumption in non-Newtonian systems are shown in Figures 6 and 7 for several test fluids but one geometry HR3 thereby elucidating the effects of shear thinning and viscoelastic behavior. Qualitatively similar trends were observed with the other geometrical arrangements investigated in this work. The generalized Reynolds number in these figures has been defined using the effective viscosity calculated using the method of Metzner and Otto (1957), that is, Eq. 2 using the Newtonian power curve in the laminar regime as a reference.

A detailed examination of the results shown in Figures 6 and 7 as well as of those not presented herein suggests that, in the absence of viscoelastic effects, laminar flow for highly shear thinning fluids persists up to somewhat larger values of the generalized Reynolds number than that for the Newtonian fluids. Therefore, a smaller torque is needed to mix shear thinning liquids in the transition regime than that for Newtonian fluids. The smaller the value of  $n$  is, the higher is the value of the Reynolds number marking the onset of the transition flow. The results obtained with the highly shear thinning and relatively inelastic 2.5% xanthan aqueous solution corroborate these assertions. Similar results have been also reported by Brito et al. (1991). For mildly shear thinning and

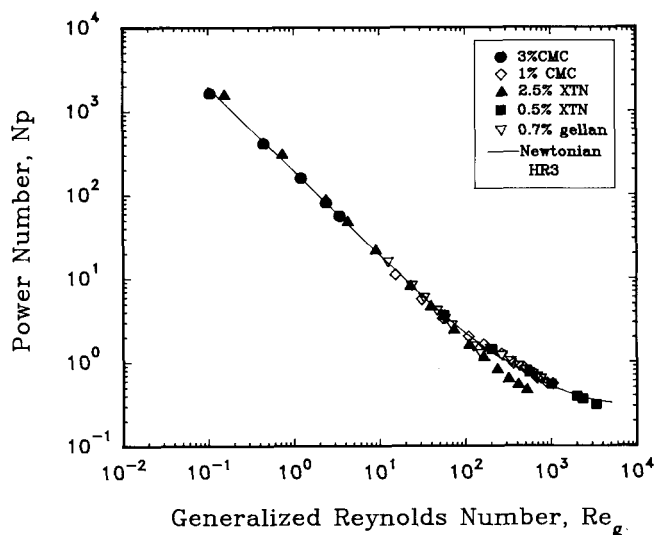


**Figure 6. Power data for the shear thinning inelastic fluids.**

inelastic fluids, the present results are virtually indistinguishable from the Newtonian power curve in the transition regime. This observation is also consistent with the finding of previous studies (Harnby et al., 1992).

For the mixing of viscoelastic liquids, the values of power number are in line with the Newtonian curve only for low values of the Reynolds number. For these low values, the corresponding values for the Weissenberg number [ $Wi = (\Psi_1/\eta_e)N$ ] are small and it is expected to show little effect on the power consumption. With an increase in the velocity (hence  $Re$  and  $Wi$ ), the viscoelastic effects become more and more pronounced and the more elastic the fluid is, the sooner is the departure from the Newtonian curve. In other words much greater power is required to mix highly viscoelastic systems than Newtonian fluids of comparable viscosity, and with increasing elasticity of the fluids the value of the Reynolds number is smaller up to which the laminar flow is seen to exist. These results are in line with the findings of Prud'homme and

**Table 3. Comparison of Experimental Data of  $K_p$  with Literature**

Geometry	Experimental (This Work)	Chavan and Ulbrecht (1973)	Yap et al. (1979)	Shamlou and Edwards (1985)
HR1	164.1	180.9	136.2	226.7
HR2	132.2	176.7	103.0	229.5
HR3	192.2	206.8	129.8	253.9
HR4	160.5	165.5	136.2	213.2
HR5	120.1	150.9	80.4	203.9
HR6	176.8	204.6	127.9	249.6

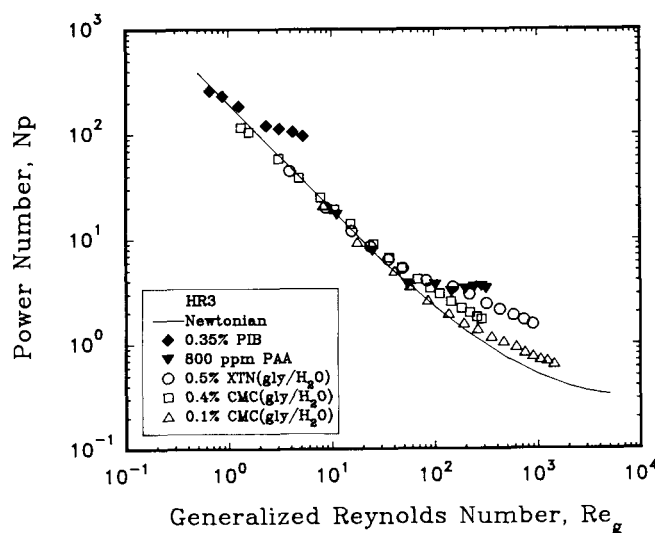


**Figure 7. Power data for the viscoelastic fluids.**

Shaqfeh (1984) and Carreau et al. (1992) for impellers of different types, as well as with the observations of Brito et al. (1991) for similar agitators. In this context, the results obtained with the two Boger (nearly shear independent elastic) fluids are particularly informative, which illustrate the aforementioned phenomena unequivocally.

Figure 8 shows the effect of the Weissenberg number on the power number. Note the qualitatively similar behavior exhibited by different types of fluids. Bearing in mind the opposing effects of shear thinning and viscoelasticity, the results for the Boger fluids (0.35% PIB and 800 ppm PAA) are seen to deviate at rather small values of the Weissenberg number. The fact that the results for the highly shear thinning and viscoelastic xanthan solution in glycerol conform the Newtonian behavior up to rather large values of the Weissenberg number ( $\sim 0.1$ ) suggests that shear thinning delays the onset of viscoelastic effects. Qualitatively similar trends have been documented by Brito et al. (1991) for a helical ribbon agitator and by Nienow et al. (1983) for a Rushton type agitator. However, there does not appear to be a simple method of predicting *a priori* the onset of departure from the Newtonian curve in this complex flow configuration. It should be mentioned here that the point at which the results begin to veer away from the Newtonian curve also coincides with that at which the rod climbing phenomenon is observed in mixing experiments. Obviously, the fluid's elasticity is responsible for changes in the flow patterns, as discussed by Ulbrecht and Carreau (1985). To quantitatively describe the effects of flow pattern changes on the power consumption in such a complex flow system is, however, impossible without a detailed investigation of the flow field. Qualitatively, we suggest that more energy is required to mix viscoelastic fluids, because the flow in a mixing vessel is highly transient and partly extensional. Viscoelastic fluids are known to exhibit large stress overshoots in transient experiments, and their extensional viscosity could be quite large compared to their shear viscosity (see Bird et al., 1987).

In view of the opposing effects of shear thinning and viscoelastic behavior on power, it is conceivable that under appropriate circumstances, the results for a shear thinning viscoelastic liquid may not deviate from the corresponding Newtonian curve. This expectation is borne out by the results obtained with the highly shear thinning and viscoelastic 0.5%

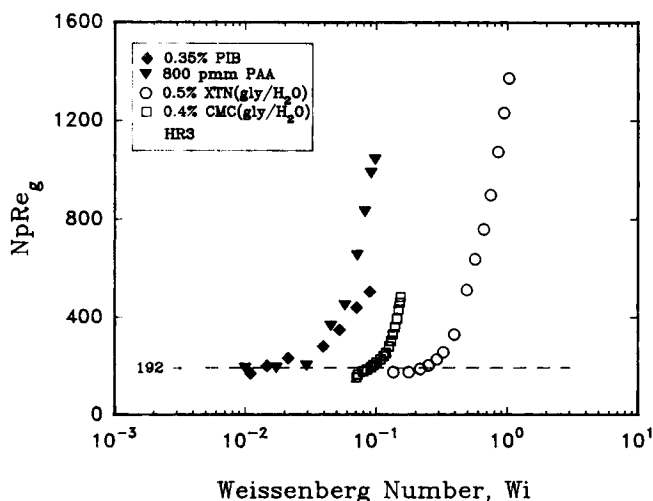


Figure 8. Variation of  $NpRe_g$  with Weissenberg number.

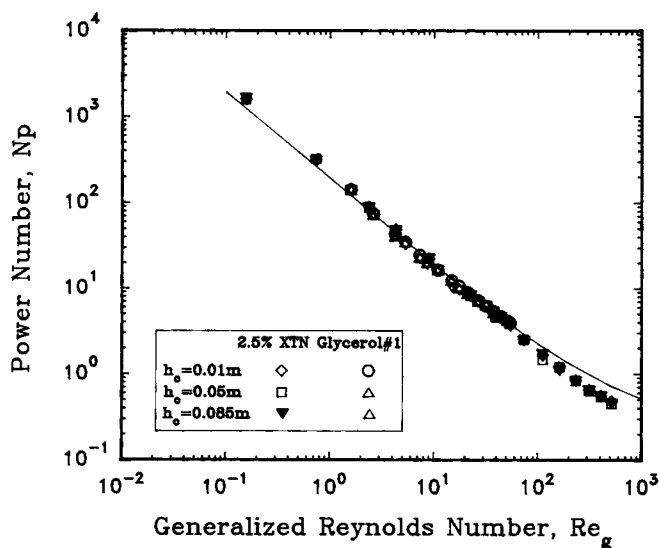


Figure 9. Bottom effect on the power consumption.

xanthan solution in glycerol. Only at sufficiently high values of the Reynolds number (and thus Weissenberg number) do the results begin to veer away from the Newtonian curve. Finally, Figure 9 shows that the clearance between the impeller and the bottom of the vessel exerts virtually no influence on the power consumption for a series of Newtonian and non-Newtonian fluids using the impeller HR3. One would intuitively expect similar results for other geometries too.

### Predicted and experimental effective shear rate

Figures 10 and 11 show representative results of  $k_s$  (calculated using the method of Metzner and Otto (1957)) as a function of the generalized Reynolds number  $Re_g$  for one agitator geometry (HR3). The  $k_s$  value is found to be constant only in the laminar flow regime for purely viscous (that is, inelastic) fluids and for very low Reynolds numbers in the case of the

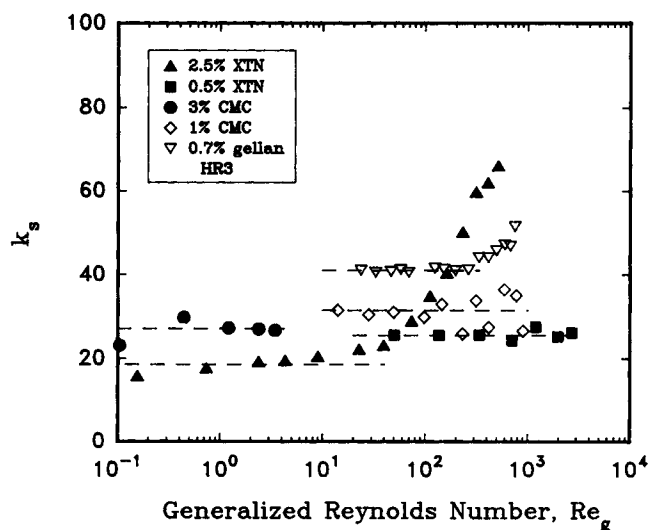


Figure 10. Variation of  $k_s$  with generalized Reynolds number for the shear thinning inelastic fluids.

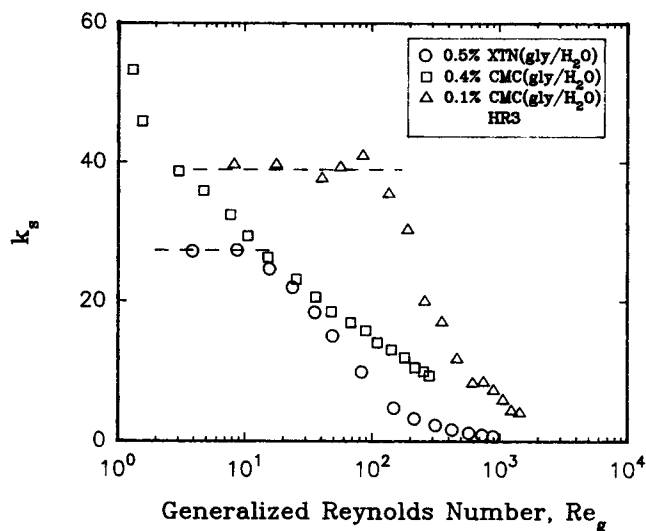


Figure 11. Variation of  $k_s$  with generalized Reynolds number for the viscoelastic fluids.

viscoelastic liquids, that is, before the departure from the laminar regime. For the 0.4% CMC in glycerol/water, no constant  $k_s$  could be obtained within the experimental range.

Beyond the laminar flow and/or beyond the point of departure, the relationship between  $k_s$  and  $Re_g$  seems to be strongly dependent upon the rheological characteristics of the liquid. Broadly speaking,  $k_s$  calculated using the Metzner-Otto (1957) method is strongly dependent on the generalized Reynolds number  $Re_g$ . For highly shear thinning fluids the increase of  $k_s$  at high Reynolds number is due to the extension of the laminar regime. For viscoelastic fluids, on the contrary, the decrease is caused by early departure from the generalized Newtonian power curve. As expected,  $k_s$  is somewhat dependent on the agitator geometry. Figure 12 reports the values of  $k_s$  for the non-Newtonian fluids used in this work determined

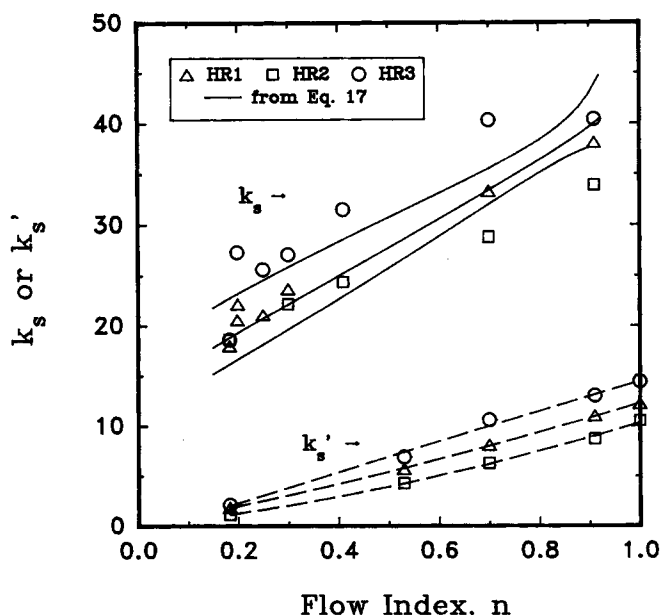


Figure 12. Dependence of  $k_s$  or  $k'_s$  on the flow index  $n$ .

in the laminar regime, for only three geometries to avoid overcrowding of the figure. It is obvious that in addition to geometry,  $k_s$  is quite dependent on the flow behavior index,  $n$ . This last finding is also consistent with the conclusions reached by other investigators (for example, Beckner and Smith, 1966; Yap et al., 1979; Brito et al., 1991). The increase of  $k_s$  with  $n$  is not predicted by Eq. 13 using the power constant,  $K_p$ , determined for Newtonian fluids. This will be discussed below.

Alternately, one can also predict  $k_s$  using Eq. 17, via the wall shear rate constant  $k'_s$ . The constant of proportionality  $k'_s$  is also plotted against the power law index  $n$  in Figure 12, for three geometrical configurations only. The other systems show a similar behavior. The predictions of  $k_s$  and the values calculated from the Metzner-Otto (1957) method are in close agreement. For high values of  $n$ , the predictions are quite sensitive to the  $K_p$  values and become undetermined for  $n = 1$ . These results provide a theoretical justification for the empirical approach of Metzner and Otto (1957).

The power and applicability of the approach developed herein is also demonstrated by predicting the equivalent diameter  $d_e$  using the power measurements via Eq. 13. The results are shown in Figure 13 where it is clearly seen that the value of  $d_e$  is somewhat influenced by the extent of shear thinning behavior. Although the reasons for the dependence of  $D/d_e$  on  $n$  are not immediately obvious, this can be attributed in part to the changes in flow patterns for highly shear thinning fluids as observed by Carreau et al. (1976) and recently computed by Tanguy et al. (1991). However, in spite of the slight dependence of  $D/d_e$  on  $n$ , it can be argued that the calculation of power is not very sensitive to the variation of  $D/d_e$  with  $n$ . For engineering calculations, it is quite adequate to use the value of  $(D/d_e)$  from Newtonian fluids, listed in Table 1, together with the  $k_s$  determined from Eq. 13. Figure 14 confirms this expectation: the deviations between the predicted values using the equivalent diameter for Newtonian fluids and the power data for impeller HR3 are barely noticeable. The predictions for 2.5% XTN solution coincide almost exactly

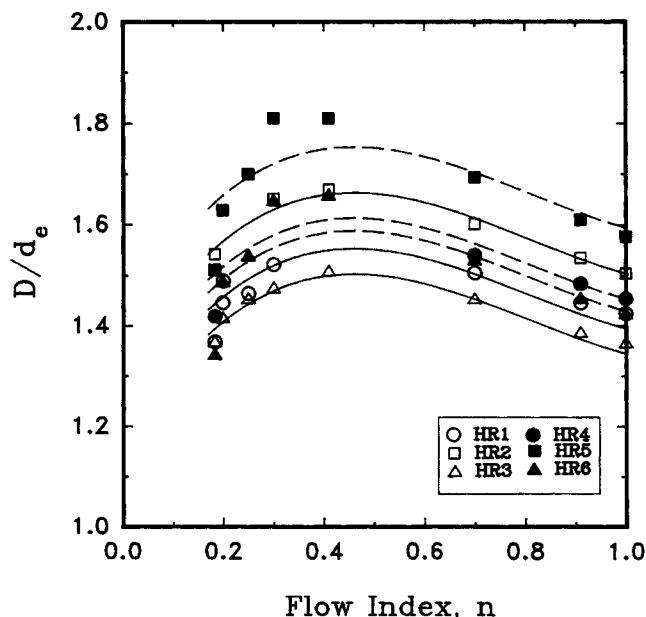
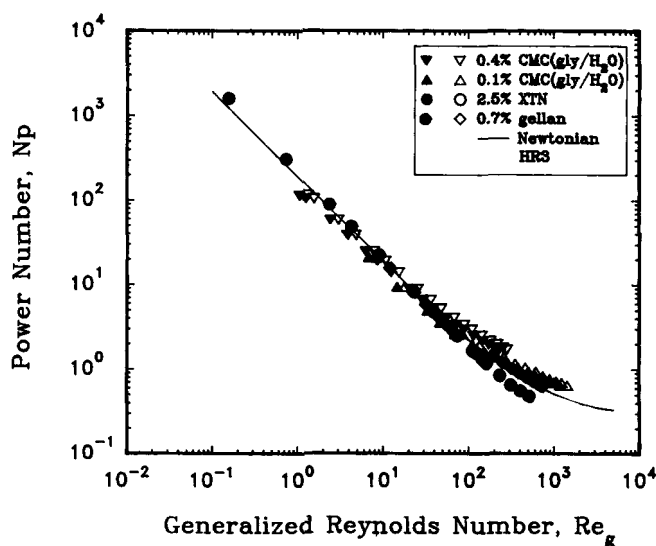


Figure 13. Dependence of  $D/d_e$  on the flow index  $n$ .





**Figure 14. Power predictions using  $d_e$  from Newtonian data (value reported in Table 1).**

Open symbols: experimental; solid symbols: predictions.

with the experimental data, so that the differences in the figure cannot be seen. For this solution,  $k_s$  is exactly predicted by Eq. 13. The results for the other geometries would be comparable. We stress that, with this approach, power consumption for mixing inelastic non-Newtonian fluids can be predicted from the Newtonian power constant,  $K_p$ .

## Conclusions

In this work, the influence of the shear thinning and viscoelastic characteristics on the power requirement for the mixing of liquids with helical ribbon agitators have been investigated. For mildly to fairly high shear thinning inelastic liquids ( $n \geq 0.25$ ), the power consumption does not deviate from the corresponding Newtonian curve in the laminar as well as in the early transition flow regime. For highly shear thinning inelastic fluids ( $n < 0.2$ ) the power number shows an extended laminar flow regime, that is, the onset of the transition regime is somewhat delayed. The viscoelastic behavior exerts an exactly opposite effect, that is, the power number for shear independent viscoelastic (Boger) fluids is well represented by the Newtonian curve only for very low values of the Reynolds number (and Weissenberg number). With increasing  $Re$ , viscoelastic effects become more pronounced and the power number is much larger than for Newtonian fluids. Conversely, these fluids exhibit a much shorter laminar flow regime than Newtonian fluids. For fluids which exhibit both shear thinning as well as viscoelastic properties, the effect of elasticity (or Weissenberg number) is less pronounced and the departures of the power number from the Newtonian curve is observed for higher Reynolds number than for the shear independent viscoelastic fluids.

Based on the analysis of Couette flow, simple semitheoretical models have also been outlined for the laminar regime herein, which in conjunction with the experimental torque values enable us to predict the effective shear rate. The functional dependence of the wall shear rate and of the effective shear rate on the flow behavior index and geometry is reported and dis-

cussed. The wall shear rate is linked with the effective shear rate in the tank estimated using the concept introduced by Metzner and Otto (1957). The proposed models can be used to predict the effective shear rate and predict the power consumption for the mixing of inelastic non-Newtonian fluids with close clearance impellers in the laminar regime. Finally, the present experimental results also suggest that the clearance between the agitator and bottom does not influence the power consumption to an appreciable extent.

## Acknowledgment

We wish to express our thanks to Professor L. Choplin and Dr. E. Brito for most appreciated suggestions and discussion. During the course of this work, R. P. Chhabra was supported by an International Exchange Visitor grant provided by NSERC (to P. J. Carreau). Also, the financial support received from the FCAR Program of the Province of Quebec is gratefully acknowledged.

## Notation

- $d_e$  = equivalent diameter of impeller, m
- $D$  = vessel diameter, m
- $h$  = impeller height, m
- $h_c$  = bottom clearance, m
- $H$  = height of liquid in the vessel, m
- $K_p$  = proportionality constant of the power number, Eq. 12
- $k_s$  = Metzner-Otto coefficient, Eq. 2
- $k'_s$  = wall shear rate constant, Eq. 16
- $m$  = power law parameter, Eq. 6,  $\text{Pa} \cdot \text{s}^n$
- $m'$  = parameter, Eq. 20,  $\text{Pa} \cdot \text{s}^n$
- $n$  = power law index, Eq. 6
- $n'$  = parameter, Eq. 20
- $N$  = impeller rotational speed,  $\text{s}^{-1}$
- $Np$  = power number,  $P/d^3 N^3 \rho$
- $N_1$  = primary normal stress differences, Pa
- $p$  = impeller pitch, m
- $P$  = power, W
- $r$  = radial coordinate, m
- $R$  = vessel radius, m
- $Re$  = Reynolds number,  $d^2 N \rho / \eta$
- $Re_g$  = generalized Reynolds number,  $d^2 N \rho / \eta_e$
- $t_1$  = Cross model parameter, Eq. 18, s
- $v_r$  = radial velocity, m/s
- $v_z$  = axial velocity, m/s
- $v_\theta$  = angular velocity, m/s
- $Wi$  = Weissenberg number,  $\Psi_1 N / \eta_e$

## Greek letters

- $\dot{\gamma}$  = shear rate  $\text{s}^{-1}$
- $\dot{\gamma}_e$  = effective shear rate,  $\text{s}^{-1}$
- $\dot{\gamma}_{\theta, \text{wall}}$  = shear rate at the vessel wall,  $\text{s}^{-1}$
- $\Gamma$  = torque exerted on the vessel wall,  $\text{N} \cdot \text{m}$
- $\eta$  = non-Newtonian viscosity,  $\text{Pa} \cdot \text{s}$
- $\eta_s$  = solvent viscosity,  $\text{Pa} \cdot \text{s}$
- $\eta_0$  = zero-shear viscosity,  $\text{Pa} \cdot \text{s}$
- $\lambda$  = characteristic elastic time, Eq. 21, s
- $\rho$  = liquid's density,  $\text{kg/m}^3$
- $\tau_{rz}$  =  $rz$ -component of stress tensor, Pa
- $\tau_{\theta z}$  =  $\theta z$ -component of stress tensor, Pa
- $\tau_{r\theta}$  =  $r\theta$ -component of stress tensor, Pa
- $\tau_{11}$  = normal stress component, Pa
- $\tau_{22}$  = normal stress component, Pa
- $\Psi_1$  = primary normal stress coefficient,  $\text{Pa} \cdot \text{s}^2$
- $\Omega$  = angular velocity of cylinder or impeller,  $\text{s}^{-1}$

## Literature Cited

- Beckner, J. L., and J. M. Smith, "Anchor-Agitated Systems: Power Input with Newtonian and Pseudoplastic Fluids," *Trans. Inst. Chem. Eng.*, **44**, 224 (1966).

- Bird, R. B., R. C. Armstrong, and O. Hassager, *Dynamics of Polymeric Liquids*, Vol. 1, Fluid Mechanics, Second ed., Wiley, New York (1987).
- Boger, D. V., and R. Binnington, "Separation of Elastic and Shear Thinning Effects in the Capillary Rheometer," *Trans. Soc. Rheol.*, **21**, 515 (1977).
- Bourne, J. R., and H. Butler, "Power Consumption of Helical Ribbon Impellers in Inelastic Non-Newtonian Liquids," *Chem. Eng. J.*, **47**, 263 (1969).
- Brito, E., J. C. Leuliet, L. Choplin, and P. A. Tanguy, "On the Effect of Shear-Thinning Behaviour on Mixing with a Helical Ribbon Impeller," *Chem. Eng. Res. & Des.*, **69**, 324 (1991).
- Carreau, P. J., I. Patterson, and C. Y. Yap, "Mixing of Viscoelastic Fluids with Helical-Ribbon Agitators-I-Mixing Time and Flow Patterns," *Can. J. Chem. Eng.*, **54**, 135 (1976).
- Carreau, P. J., J. Paris, and P. Guérin, "Mixing of Newtonian and Non-Newtonian Liquids: Screw Agitator and Draft Coil System," *Can. J. Chem. Eng.*, **70**, 1071 (1992).
- Chavan, V. V., and J. J. Ulbrecht, "Power Correlations for Close-Clearance Helical Impellers in Inelastic non-Newtonian Liquids," *Chem. Eng. J.*, **3**, 308 (1972).
- Hall, K. L., and J. C. Godfrey, "Power Consumption by Helical Ribbon Impellers," *Trans. Inst. Chem. Eng.*, **48**, T201 (1970).
- Harnby, N., M. F. Edwards, and A. W. Nienow, *Mixing in the Process Industries*, Butterworths, London (1992).
- Metzner, A. B., and J. C. Otto, "Agitation of Non-Newtonian Fluids," *AIChE J.*, **3**, 3 (1957).
- Nienow, A. W., D. J. Wisdom, and J. Solomon, "The Effect of Rheological Complexities on Power Consumption in an Aerated Agitated Vessel," *Chem. Eng. Commun.*, **19**, 273 (1983).
- Oldshue, J. Y., *Fluid Mixing Technology*, McGraw-Hill, New York (1983).
- Patterson, I., P. J. Carreau, and C. Y. Yap, "Mixing with Helical Ribbon Agitators, Part II—Newtonian Fluids," *AIChE J.*, **25**, 516 (1979).
- Prud'homme, R. A., and E. G. Shaqfeh, "Effect of Elasticity on Mixing Torque Requirements for Rushton Turbines," *AIChE J.*, **30**, 485 (1984).
- Shamlou, P. A., and M. F. Edwards, "Power Consumption of Helical Ribbon Mixers in Viscous Newtonian and Non-Newtonian Fluids," *Chem. Eng. Sci.*, **40**, 1773 (1985).
- Takahashi, K., T. Yokota, and H. Konno, "Power Consumption of Helical Ribbon Agitators in Highly Viscous Pseudoplastic Liquids," *J. Chem. Eng. Japan*, **17**, 657 (1984).
- Tanguy, P. A., R. Lacroix, F. Bertrand, L. Choplin, and E. Brito, "Mixing of Rheologically Complex Fluids with an Helical Ribbon Impeller: Experimental and 3-D Numerical Studies," *7th European Cong. on Mixing*, Brugge, Belgium, p. 507 (1991).
- Tatterson, G. B., *Fluid Mixing and Gas Dispersion in Agitated Tank*, McGraw-Hill, New York (1991).
- Ulbrecht, J. J., and P. J. Carreau, "Mixing of Viscous non-Newtonian Fluids," *Mixing of Liquids by Mechanical Agitation*, Chapter 4, J. J. Ulbrecht and G. K. Patterson, eds., Gordon and Breach, New York (1985).
- Yap, Y. C., W. I. Patterson, and P. J. Carreau, "Mixing with Helical Ribbon Agitators, Part III—Non-Newtonian Fluids," *AIChE J.*, **25**, 516 (1979).

Manuscript received Jan. 25, 1993, and revision received Mar. 24, 1993.